

5820-31
P. 34

AIRCRAFT WAKE-VORTEX MINIMIZATION BY USE OF FLAPS

Victor R. Corsiglia and R. Earl Dunham, Jr.*

Ames Research Center

SUMMARY

A survey is made of research on the alleviation of the trailing vortex hazard by altering span loading with flaps on the generator airplane. Flap configurations of the generator that shed multiple vortices were found to have wakes that dispersed by vortex merging and sinusoidal instability. Reductions of approximately 50 percent in both the wake rolling moment imposed on a following aircraft and the aircraft separation requirement were achieved in the ground-based and flight-test experiments by deflecting the trailing-edge flaps more inboard than outboard. Significantly, this configuration did not increase the drag or vibration on the generating aircraft compared to the conventional landing configuration. Ground-based results of rolling-moment measurement and flow visualization are shown, using a water tow facility, an air tow facility, and a wind tunnel. Flight-test results are also shown, using a full-scale B-747 airplane. General agreement was found among the results of the various ground-based facilities and the flight tests. Some progress has been made in identifying configurations that alleviate the wake; however, more research is required before a configuration acceptable for airline operation is found.

INTRODUCTION

The objective of the NASA wake-vortex alleviation program is to reduce the intensity of the lift-generated vortices shed by large subsonic transport aircraft so that separation distances between aircraft can be reduced during landing and takeoff. One aspect of this program has been devoted to investigating the effect on the wake of turbulence injection into the vortices

*Langley Research Center.

(refs. 1-14). In these studies, a variety of spoiler sizes and locations were considered, as well as various spline configurations. Although some of the turbulence injection devices were effective in reducing wake intensity, the penalties associated with their drag, lift, unsteady loads, and installation made them unacceptable solutions to the wake-vortex problem. Recently, however, the use of the existing spoilers on the *B-747* airplane has been found to be effective (refs. 15 and 16), and an effort is underway to reduce the associated penalties to a tolerable level (ref. 17).

An alternate approach to wake-vortex minimization is to distribute the lift on the wing so that a very diffuse wake results. This approach is attractive in that lower levels of wing profile drag would be expected compared to the use of drag devices such as a spoiler or spline. This lower drag is especially important for takeoff and the climb phase of flight. This paper discusses the use of flaps as a technique to alter span loading and includes work performed by the **NASA Ames**, Flight, and Langley Research Centers.

NOTATION

b	wingspan
c	wing local chord
\bar{c}	wing average chord
c_l	local lift coefficient
c_l	rolling-moment coefficient
C_D	total drag coefficient
C_L	total lift coefficient
C_M	total pitching-moment coefficient
D	vortex spacing (see fig. 11)

i_t	horizontal stabilizer incidence
r	vortex radius
t	time
Δt	time increment
U_∞	free-stream velocity
V_θ	vortex swirl velocity
x	downstream distance
Y	spanwise distance
α	angle of attack
η	$= 2y/b_g$
$30^\circ/0^\circ$	indicates inboard flap deflected 30° and outboard flap deflected 0° typically

Subscripts

f	follower model
g	generator model

RELATIONSHIP BETWEEN SPAN LOADING AND VORTEX-WAKE INTENSITY

Theoretical

Significant progress was made in understanding the relationship between span loading on the generating wing and the structure of the downstream vortex wake when the Betz method (ref. 18) was adopted by several investigators. The wake rollup procedure described by Betz in 1932 received little attention until Donaldson (refs. 19 and 20) showed that the swirl velocity distribution calculated in this way compared favorably with measurements. Mason and Marchman (ref. 21) applied the Betz method to a series of tapered wings and

concluded that the trailing vortex became more intense as the vorticity was concentrated on the outer portion of the wing. A similar conclusion was drawn by Brown (ref. 22), who applied the Betz theory to a parabolically loaded wing. Rossow (ref. 23) applied the Betz method to a wide range of wing span loadings. Figure 1 is a sample of his results. The swirl velocity is seen to be significantly reduced in panels (b), (c), and (d) of the figure as compared to panel (a), which corresponds to elliptic span loading. Rossow (ref. 24) then extended his analysis to more complicated configurations by use of a time-dependent point-vortex model that also satisfied the Betz invariants. He found that (i) span loadings could be tailored to produce a very diffuse wake and (ii) by shedding multiple vortices in the wake, strong interactions between vortices could occur which would disperse the vorticity.

Experimental

Rorke, Moffitt, and Ward (ref. 25) found that vortex swirl velocity in the wake of a rectangular wing could be significantly reduced by installing an ogee wingtip that reduced the wingtip loading. A similar conclusion was obtained by McCormick and Padakannaya (ref. 26) in their study of the effect of a drooped wingtip. Rossow et al. (ref. 12) showed that swirl velocities could be reduced by tailoring for an optimum span loading by use of a segmented trailing-edge flap on a swept wing (fig. 2). However, the rolling moment imposed on a following model aligned with the vortex was found, in some cases, to be increased as a result of tailoring the loading, depending on the span of the follower relative to the span of the generator. Ciffone and Orloff (ref. 27) conducted further studies using the same design of swept wing as in reference 12. They found that when multiple vortices were shed in the wake, strong interactions occurred between some vortices. However, other vortices persisted in the wake and resulted in swirl velocities as high as those found in the wake of conventional configurations.

USE OF FLAPS ON THE B-747 AIRPLANE

To coordinate the activities of the various NASA centers in the wake-vortex minimization effort, a common objective was adopted. The generating

wing was agreed to be that of a B-747 airplane and the following wings would be representative of a Learjet and a DC-9 airplane for the lightweight (<12,500 lb) and medium-sized followers, respectively. Particular interest was focused on those modifications of the generator which were sufficiently minor to be regarded as retrofit modifications.

In view of research work on the effect of span loading (discussed previously), an obvious possibility for consideration on the generator was to retract the outboard flap with the inboard flap left at the landing setting (figs. 3 and 4). The generator was equipped with two spanwise segments of triple-slotted, trailing-edge flaps capable of high lift. Figure 5 shows the span loadings produced by various flap settings of the generator using a vortex lattice method for the wing and flaps, including the effect of camber and twist, but without fuselage or tail. Note that the conventional flaps 0" and takeoff configurations have approximately elliptical span loadings and hence would be expected to shed a single vortex from each wingtip. With the conventional landing configuration, some additional sharp gradients in loading are evident at the flap edges from which discrete vortices might originate. However, with the outboard flap retracted (30°/0°),¹ these gradients are more pronounced and three vortices from each wing would be expected, that is, one from each flap edge and one from the wingtip.

Ground-Based Measurement

Flow visualization - Dunham (ref. 9) conducted experiments in a water-tow facility (owned and operated by Hydronautics Inc. under contract to Langley Research Center) where the generator model was towed underwater along a long channel. He observed (fig. 6) that when the outboard flap was retracted, the wingtip and flap outboard vortex interacted and merged to form a single diffuse vortex pair aft of about 15 spans downstream. Additional flow visualization studies (refs. 28-32) were conducted using an

¹The notation 30°/0°, for example, is used to indicate 30" inboard flap deflection and 0" outboard flap deflection; 30" is the nominal angle used to designate the configuration for landing (5" for takeoff). The actual deflection of the various flap panels appears in figure 3.

air-tow channel, water-tow channel (owned and operated by the Univ. of California under contract to Ames Research Center) (fig. 7), wind tunnel, and full-scale flight test (fig. 8). From all these studies, the picture of the wake appearing in figure 9 emerged. With the conventional landing configuration aft of about 2 spans downstream, the wake consisted of two intense counterrotating cores that very slowly diffused their vorticity. In contrast, the wake of the configuration with the outboard flap retracted and the inboard flap set to the landing deflection consisted of three vortices per side, one from each flap edge and one from the wingtip. The vortex that was most intense and well defined originated at the flap outboard edge. The two weaker vortices left the wingtip and flap inboard edge, respectively. The pattern rotated as it moved downstream, with the tip vortex passing over the flap vortices so that, by about 13 spans downstream, it had moved to a position between the flap vortices. The flap and tip vortices ultimately merged. Following this merger, a very diffuse wake remained. In addition to the vortices shown in figure 9, Ciffone and Lonzo (ref. 29) noted that the horizontal tail vortices rapidly merged with the flap vortices.

Vortex merging - The vortex merging phenomenon is a mechanism for dispersing the vorticity in the wake. It was generally observed, for example, that a single vortex pair in isolation persisted as an organized vortex with a small core, whereas it was found that the wake would disperse rapidly if (i) multiple vortex pairs were shed with initially large spacing and (ii) the self-induced wake velocities convected these vortices into close proximity. As shown in figure 7, the wingtip and flap vortices are convected into close proximity between $x/b_g = 1.5$ and $x/b = 13$. Next the vorticity of the weak vortex (tip) is convected into an annulus around the strong vortex (flap). This convection is sketched schematically in figure 10. Here the vortical region of the weak vortex is taken to be circular at time zero. In the time increments shown, this region is distorted because of the velocity of the strong vortex. When the two vortices are of comparable strength, the core region is elongated in both vortices. Furthermore, the elongation of the core will result in additional distortion because of self-induced velocities (ref. 33).

The rolling moment on a following airplane for fully merged vortices would be expected to be below that for the conventional configuration at the same lift Coefficient of the generator. For example, consider the two idealized span loadings sketched in figure 11. For the modified configuration, the wingtip and flap vortices are assumed to merge into a single circular vortex core with uniformly distributed vorticity (i.e., Rankine vortex). The circulation and core diameter of this merged vortex can be obtained from vortex invariants (ref. 18). The rolling-moment coefficient on the follower in the wake of this merged vortex, as well as in the wake of the single vortex of the conventional configuration, can be computed by use of the method discussed in reference 12 or 24 for a given lift coefficient of the generator. This result is shown in figure 11 as a function of the spacing between the two vortices of the modified configuration. For vortex spacing in excess of 0.3 of the semispan, the reduction in the rolling-moment coefficient behind the modified configuration compared with the conventional configuration is substantial. This simplified example illustrates one mechanism for dispersing the wake. In an actual wake, the vortices before merger have distributed vorticity, and there are vortices of opposite sense from the inboard edges of the flap and the horizontal stabilizer. All these vortices must be considered in predicting the downstream wake and rolling moment on a follower. Rossow (ref. 33) has conducted additional theoretical research on the conditions for the merger of multiple vortices.

Rolling moment on the follower - Experiments were conducted in the Ames 40-by 80-Foot Wind Tunnel in which the rolling moment was measured on a following model held fixed in the wake of the generator model (figs. 3 and 12). Figure 13 shows the variation of the rolling-moment coefficient with the circulation of the trailing vortex for the conventional flap settings of the generator (ref. 30) at 13.6 spans downstream of the generator. Also shown is the corresponding measurement in the wake of a supersonic transport model (ref. 34). The rolling moment increases nearly linearly with $\Gamma/b_g U_\infty$, as predicted (ref. 12) for the case when the vorticity distribution remains unchanged and only the magnitude changes. This result is expected because the shape of the span-load distribution is nearly independent of lift over the range of angle of attack tested and, for these configurations, the vortex

structure is determined by the span-load distribution (ref. 18). For figure 13, $\Gamma/b_g U_\infty$ was obtained from C_{Lg} by assuming elliptic loading. Note in figure 13 that the various configurations lie on approximately the same curve, which implies that the change in the vortex structure for the configurations shown is sufficiently small that the change in rolling moment could not be detected. When the outboard flap of the B-747 model was retracted (figs. 14(a) and (b)), a greater than 50-percent reduction in rolling moment was measured for the smaller follower model. With the larger follower model, the reduction in rolling moment was less. For comparison, typical values for the roll control capability for the Learjet and DC-9 are also presented in figure 14 and, at $C_{Lg} = 1.2$, the imposed rolling-moment coefficient about equals the capability of the Learjet and slightly exceeds the capability of the DC-9. The nominal value of C_{Lg} for the B-747 in the conventional landing configuration lies between 1.2 to 1.4.

Experiments were also conducted in the Hydronautics Inc. water-tow facility (ref. 9) using follower and generator models identical to those used in the wind-tunnel tests discussed previously. In these water-tow experiments, the follower and generator models were towed at the same speed, with the follower model held fixed at various lateral and vertical positions in the wake. By use of this technique, substantially greater downstream distances could be obtained compared to the wind-tunnel experiments. Results for the variation of C_{zf} with downstream distance appear in figures 14 (c) and (d). Also shown are comparable wind-tunnel and air-tow facility data. There is general agreement on the effectiveness of retracting the outboard flap as a technique to reduce the wake rolling moments. However, the water-tow facility data show that the effectiveness for the smaller follower (fig. 14(c)) occurs farther downstream compared with the wind-tunnel results. This difference may result from either a higher turbulence level in the wind tunnel as compared to the water-tow facility or the effect of the water tank boundaries on the paths of the vortices.

Drag, angle of attack, and pitching moment on the generator - The forces and moments on the generator were measured for the 30°/30° and 30°/0° configurations (ref. 14) (fig. 15). The effect of retracting the outboard flap

on drag was small. The change in angle of attack to maintain a lift coefficient $C_{Lg} = 1.2$ was about 3.5° (trimmed). In aircraft operation, however, this lift loss due to the $30^\circ/0^\circ$ configuration would require compensation by either an increase in aircraft angle of attack or airspeed or a combination of these variables. The effect of retracting the outboard flap on the pitching-moment characteristics is to require an additional 5° of tail incidence for trim and to reduce longitudinal static stability, $(-\partial C_M / \partial C_{Lg})$, about 13 percent at $C_{Lg} = 1.2$. In airline operation, this effect on the pitching-moment characteristics would probably require that the aft limit of the center-of-gravity location be moved forward from its present location.

Flight Test

As a result of the ground-based studies discussed above, flight tests were conducted using a full-scale B-747 airplane to generate the wake and a Learjet and T-37B airplanes to probe the wake (refs. 31, 32, and 35). Figure 16 is a summary of pilot qualitative separation requirement for the follower airplane. With the landing gear retracted to correspond to the ground-based experiments, the separation requirement was reduced substantially for the $30^\circ/1^\circ$ configuration² compared to the $30^\circ/30^\circ$ configuration (fig. 16(a)). Lowering the landing gear, however, increased the separation requirement for all configurations and especially for the $30^\circ/1^\circ$ configuration. Sideslip was also found to adversely affect the wake alleviation when the landing gear was up (fig. 16(b)).

Flow visualization obtained during the flight test provided some insight into the cause of the landing gear effect. Figure 17 shows the smoke trails from the B-747 airplane for the $30^\circ/1^\circ$ configuration with the landing gear both up and down. With the landing gear up, a well-defined vortex pair was shed from the inboard edge of the flaps and these vortices underwent large-amplitude sinusoidal interactions. With the landing gear deployed, these same vortices appeared to be more diffuse, and no such interactions were seen.

²For certain mechanical reasons, the outboard flap of the B-747 airplane was retracted only to 1° instead of 0° . It is felt that this difference is insignificant.

The flap inboard vortex with the landing gear up did not appear as sharp in any of the ground-based visualization experiments as it appears in figure 17. However, this apparent lack of agreement with the model tests is probably not significant since the effect of the landing gear was also measured in the ground-based experiments. Recently, Leonard (ref. 36) modeled this flow using a three-dimensional, time-dependent inviscid calculation with six concentrated vortices. His results, using a similar configuration (fig. 18), indicate that the sinusoidal oscillations observed in flight also appear in the computed results.

The rolling moment imposed on the following aircraft was obtained by subtracting the effects due to ailerons, sideslip, etc., from the measured roll acceleration during a vortex encounter. This result (ref. 32) for the configuration with the landing gear up appears in figure 19. Also shown for comparison are the results from the ground-based facilities presented above, which correspond to a rectangular wing follower whose span and aspect ratio were scaled to the aircraft used in the flight tests. Excellent agreement was obtained for the configuration with the outboard flap retracted. With the conventional landing configuration (flaps $30^\circ/30^\circ$), the ground-based rolling moment lies in the lower range of the flight-measured values, depending on the procedure used to extrapolate the ground-based results to the downstream distances tested in flight.

INTERFERENCE OF LANDING GEAR WITH WAKE ALLEVIATION

The basic factors that cause the landing gear to interfere with the vortex wake are still not fully understood. As discussed above, it appears from figure 17 that the effect of the landing gear is to diffuse the flap inboard vortex. Therefore, a vortex generator (figs. 4 and 20) which was designed to shed a strong vortex at the same location and sense as each of the flap inboard vortices when the landing gear was down was tested in the Hydronautics Inc. water tow facility. The results without the vortex generator installed (fig. 21) show a substantial increase in rolling moment due to the landing gear for the $30^\circ/0^\circ$ flap configuration similar to those achieved in the flight tests. With the vortex generator installed, the

rolling-moment reduction due to flaps was insensitive to the presence of the landing gear. Patterson and Jordan (ref. 28) (fig. 22), in their air-tow facility studies, were able to produce an increase in rolling moment, with the landing gear removed, equal to the gear effect by either placing end plates at the inboard edges of the flap or by extending the flap inboard across the fuselage. A possible explanation of these results is that both the end plate and the fuselage flap diffused the flap inboard vortex. Further research is required to directly measure the flap inboard vortex axial and swirl velocities to determine the actual role of this vortex on the alleviation of the wake. Ciffone and Lonzo (ref. 29) observed in their water-tow studies that the concentrations of dye and the vortex trajectories were different between landing gear up and down with the $30^\circ/0^\circ$ flap configuration. They then studied an alternate configuration that appeared to alleviate the wake and to be insensitive to the presence of the landing gear. This configuration was obtained by setting both the inboard and outboard flaps to **30"** deflection and removing the inboard 30 percent of the inboard flap. Studies of this configuration are continuing.

CONCLUDING REMARKS

Certain span-load distributions produce less intense wakes than others. An approximately 50-percent reduction in both the wake rolling moment imposed on a following aircraft and aircraft separation requirement was achieved in the ground-based and flight-test experiments by deflecting the trailing-edge flaps more inboard than outboard. Significantly, this configuration did not increase the drag or vibration on the generating aircraft compared to the conventional landing configuration. However, further research is required to obtain a configuration with an alleviated wake that is acceptable for airline operation.

Another major conclusion derived from the investigations summarized here is that wake-vortex experiments conducted in ground-based facilities produce results that correlate well with full-scale flight-test results. It was found that there was general agreement in both the flow visualization and the

rolling moment imposed on a following aircraft between flight-test and ground-based experiments.

REFERENCES

1. Chigier, N. A.; and Corsiglia, V. R.: Tip Vortices-Velocity Distributions, NASA TM X-62, 087, 1971
2. Chigier, N. A.; and Corsiglia, V. R.: Wind-Tunnel Studies of Wing Wake Turbulence. *J. Aircraft*, vol. 9, no. 12, 1972, pp. 820-825.
3. Corsiglia, V. R.; Schwind, R. K.; and Chigier, N. A.: Rapid Scanning Three-Dimensional Hot-wire Anemometer Surveys of Wing-Tip Vortices, *J. Aircraft*, vol. 10, no. 12, 1973, pp. 752-757.
4. Orloff, K. L.; and Grant, G. R.: The Application of a Scanning Laser Doppler Velocimeter to Trailing Vortex Definition and Alleviation. AIAA Paper 73-680, 1973 (see also NASA TM X-62,243, 1973).
5. Orloff, K. L.: Trailing Vortex Wind-Tunnel Diagnostics with a Laser Velocimeter, *J. Aircraft*, vol. 11, no. 8, 1974, pp. 477-482.
6. Corsiglia, V. R.; Jacobsen, R. A.; and Chigier, N. A.: An Experimental Investigation of Trailing Vortices Behind a Wing With a Vortex Dissipator. *Aircraft Wake Turbulence and Its Detection*, edited by J. Olson, A. Goldberg, and M. Rogers, Plenum Press, New York, 1971, pp. 229-242.
7. Wentz, W. H., Jr.: Evaluation of Several Vortex Dissipators by Wind Tunnel Measurements of Vortex-Induced Upset Loads. Wichita State Univ. Aeronautical Rept. 72-3, 1972.
8. Kirkman, K. L.; Brown, C. E.; and Goodman, A.: Evaluation of Effectiveness of Various Devices for Attenuation of Trailing Vortices Based on Model Tests in a Large Towing Basin, NASA CR-2202, 1973.
9. Dunham, E. R., Jr.: Model Tests of Various Vortex Dissipation Techniques in a Water Towing Tank, Langley Working Paper, LWP-1146, Jan. 1974.

10. Hastings, E. C., Jr.; Shanks, R. E.; Champine, R. A.; Copeland, W. L.; and Young, D. C.: Preliminary Results of Flight Tests of Vortex Attenuating Splines. NASA TM X-71,928, 1974.
11. Croom, Delwin R.: Low-Speed Wind-Tunnel Investigation of Forward-Located Spoilers and Trailing Splines as Trailing-Vortex Hazard-Alleviation Devices on an Aspect-Ratio-8 Wing Model. NASA TM X-3166, 1975.
12. Rossow, V. J.; Corsiglia, V. R.; Schwind, R. G.; Frick, J. K. D.; and Lemmer, O. J.: Velocity and Rolling-Moment Measurements in the Wake of a Swept-Wing Model in the 40- by 80-Foot Wind Tunnel. NASA TM X-62,414, 1975.
13. Patterson, J. C., Jr.: Vortex Attenuation Obtained in the Langley Vortex Research Facility. J. Aircraft, vol. 12, no. 9, Sept. 1975, pp. 745-749.
14. Croom, D. R.; and Dunham, E. R., Jr.: Low-Speed Wind-Tunnel Investigation of Forward-Located Spoiler, and Trailing Splines as Trailing-Vortex Hazard-Alleviation Devices, NASA TN D-8133, 1975.
15. Croom, D. R.: Low-Speed Wind-Tunnel Investigation of Various Segments of Flight Spoilers as Trailing-Vortex Hazard-Alleviation Devices on a Transport Aircraft Model, NASA TN D-8162, 1976.
16. Croom, D. R.: The Development of the Use of Spoilers as Vortex Attenuators. NASA Symposium on Wake Vortex Minimization, Washington, D.C., Feb. 25-26, 1977.
17. Corsiglia, V. R.; and Rossow, V. J.: Wind-Tunnel Investigation of the Effect of Porous Spoilers on the Wake of a Subsonic Transport Model, NASA TM X-73,091, 1976.
18. Betz, A.: Behavior of Vortex Systems, NACA TM 713, Z. Angew. Math. Mech. transl., vol. XII, 3, 1932.
19. Donaldson, C. du P.: A Brief Review of the Aircraft Trailing Vortex Problem, Rept. AFOSR-TR-71-1910, July 1971.

20. Donaldson, C. du P.; Snedeker, R. S.; and Sullivan, R. D.: A Method of Calculating Aircraft Wake Velocity Profiles and Comparison With Full-Scale Experimental Measurements, *J. Aircraft*, vol. 11, Sept. 1974, pp. 547-555.
21. Mason, W. H.; and Marchman, J. F., III: Far-field Structure of an Aircraft Trailing Vortex, Including Effects of Mass Injection. NASA CR-62,078, 1972.
22. Brown, C. E.: Aerodynamics of Wake Vortices. *AIAA J.*, vol. 11, no. 4, April 1973, pp. 531-536.
23. Rossow, V.: On the Inviscid Rolled-up Structure of Lift-Generated Vortices. *J. Aircraft*, vol. 10, no. 11, Nov. 1973, pp. 647-650.
24. Rossow, V. J.: Theoretical Study of Lift-Generated Vortex Wakes Designed to Avoid Rollup. *AIAA J.*, vol. 13, no. 4, April 1975, pp. 476-484.
25. Rorke, J. B.; Moffitt, R. C.; and Ward, J. F.: Wind-Tunnel Simulation of Full-scale Vortices. A.H.S. Paper 623, May 1972.
26. McCormick, B. W.; and Padakannaya, R.: The Effect of a Drooped Wing Tip on Its Trailing Vortex System. *Aircraft Wake Turbulence and Its Detection*, edited by J. Olson, A. Goldberg, and M. Rogers, Plenum Press, New York, 1971, pp. 157-70.
27. Ciffone, D. L.; and Orloff, K. L.: Far-Field Wake-Vortex Characteristics of Wings, *J. Aircraft*, vol. 12, no. 5, May 1975.
28. Patterson, J. C., Jr.; and Jordan, F. L., Jr.: An Investigation of the Increase in Vortex Induced Rolling Moment Associated with Landing Gear Wake. NASA TM X-72,786, 1975.
29. Ciffone, D. L.; and Lonzo, C., Jr.: Flow Visualization of Vortex Interactions in Multiple Vortex Wakes Behind Aircraft. NASA TM X-62,459, 1975 (see also *Vortex Interactions in Multiple Vortex Wakes Behind Aircraft*, Preprint 76-62, 14th Aerospace Sciences Meeting, Jan. 26-30, 1976, Washington, D.C.).

30. Corsiglia, V. R.; Rossow, V. J.; and Ciffone, D. L.: Experimental Study of the Effect of Span Loading on Aircraft Wakes, NASA TM X-62,431, 1975.
31. Barber, M. R.: Vortex Attenuator Flight Experiments, NASA Symposium on Wake Vortex Minimization, Washington, D.C., February 25-26, 1977.
32. Smith, H. J.: A Flight Test Investigation of the Rolling Moments Induced on a T 37B Airplane in the Wake of a B-747 Airplane. NASA TM X-56,031, 1975.
33. Rossow, V. J.: Inviscid Modeling of Aircraft Trailing Vortices. NASA Symposium on Wake Vortex Minimization, Washington, D.C., February 25-26, 1977.
34. Rossow, V. J.; Corsiglia, V. R.; and Phillippe, J. J.: Measurements of the Vortex Wakes of a Subsonic- and a Supersonic-Transport Model in the 40- by 80-Foot Wind Tunnel, NASA TM X-62,391, 1974.
35. Tymczyszyn, J. J.; and Barber, M. R.: Recent Wake Turbulence Flight Test Programs. Paper presented at the 18th Annual Symposium of the Society of Experimental Tests Pilots, September 26, 1974, Beverly Hills, Calif.
36. Leonard, A.: Numerical Simulation of Interacting, Three-Dimensional Vortex Filaments, Proceedings of the 4th International Conference on Numerical Methods in Fluid Dynamics, Boulder, Colorado, June 24-28, 1974, pp. 245-250; also published in Lecture Notes in Physics, vol. 35, Springer-Verlag, Berlin, 1975.

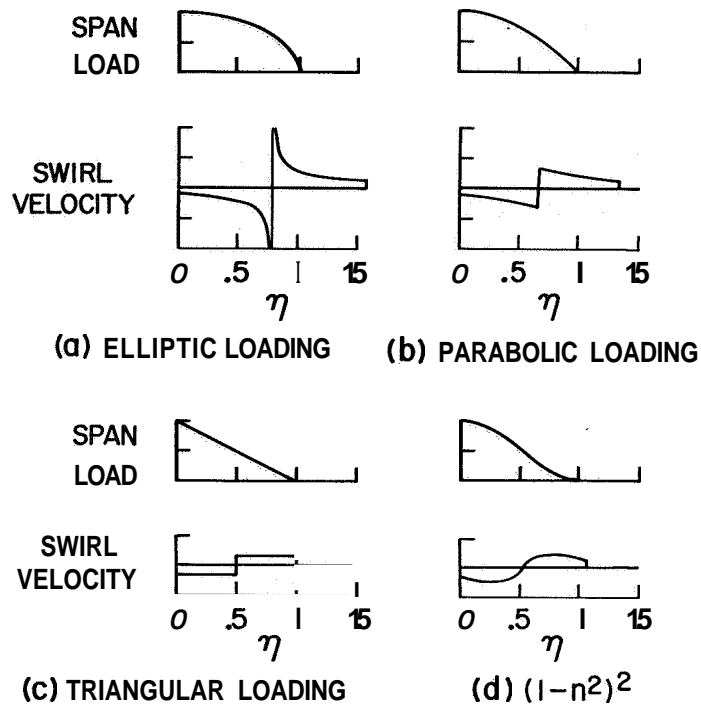


Figure 1.-, Predicted swirl velocity in the downstream wake for various span-load distributions using the Betz method (ref. 18) by Rossow (ref. 23).

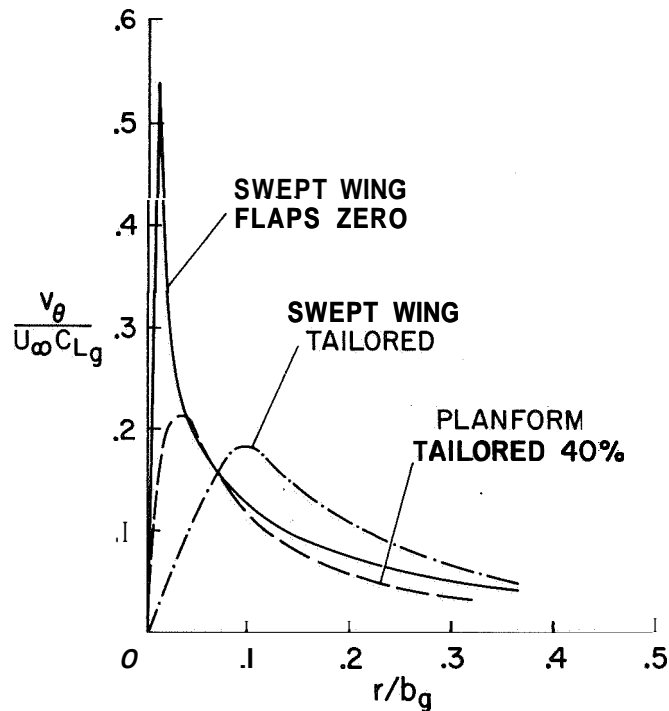
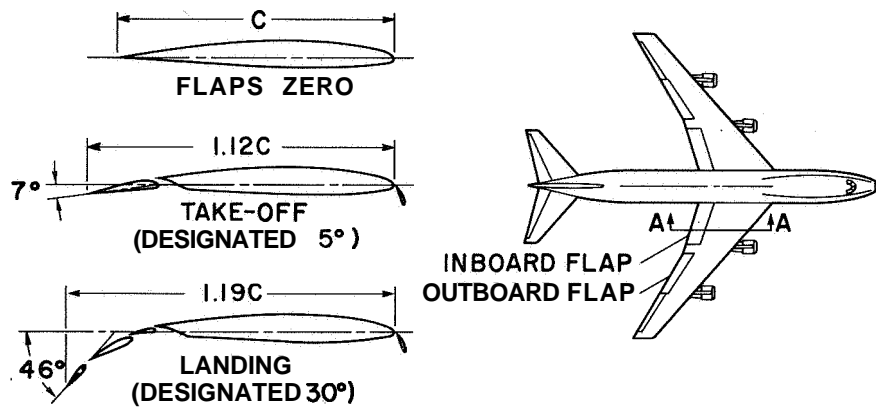
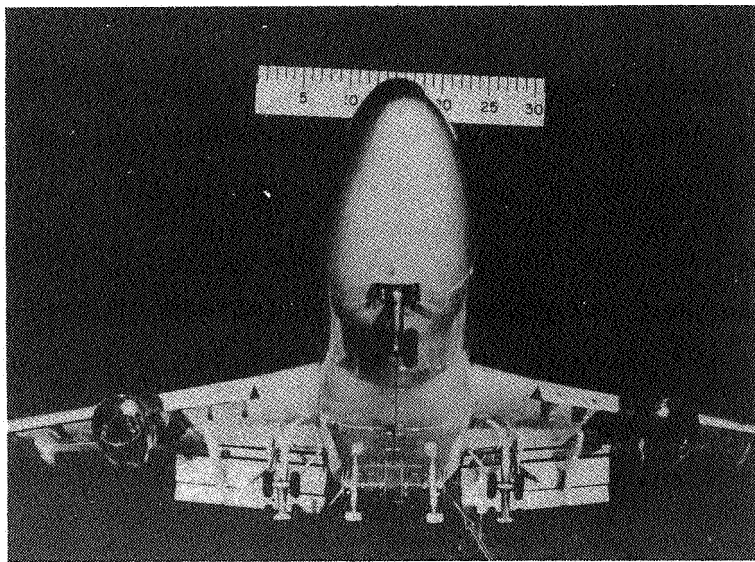


Figure 2.- Measured swirl velocity distribution in the downstream vortex for two configurations whose span loadings have been tailored according to the method described in reference 24 to produce a diffuse vortex as compared to a swept wing with flaps undeflected (ref. 12).



SECTION A-A DETAILS

Figure 3.- Sketch of the B-747 model.



**VORTEX GENERATOR AT
~ 45° TO VERTICAL**

Figure 4.- Photograph of the B-747 model (dimensions in cm).

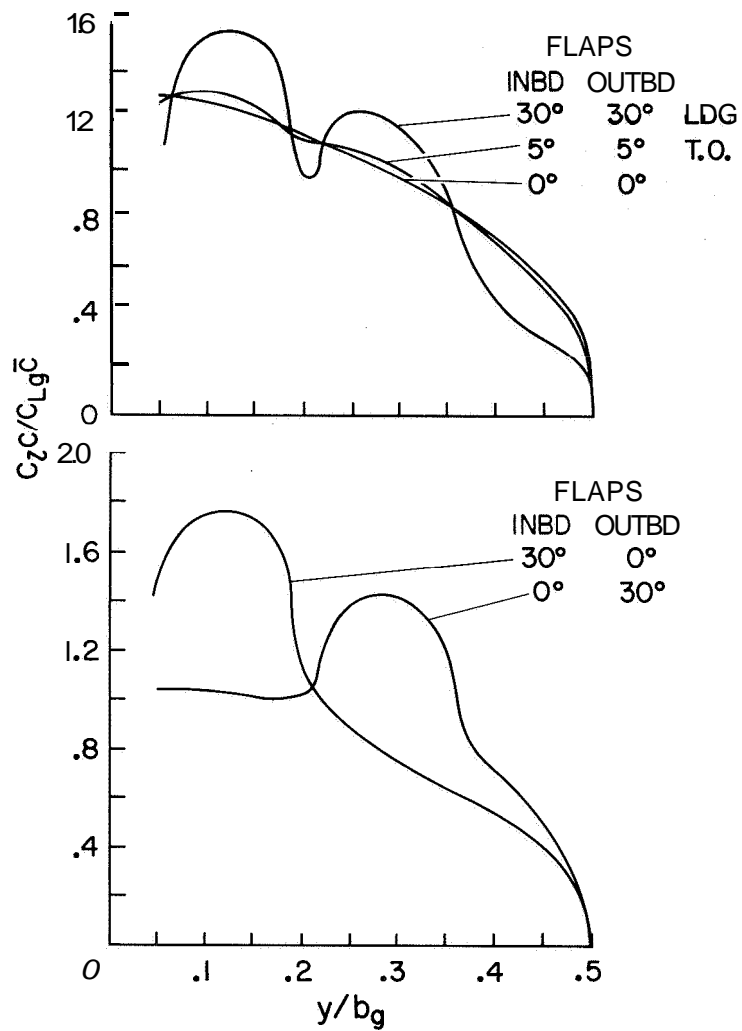


Figure 5.- Predicted variation of span loading on the **B-747** model for various settings of the inboard and outboard trailing-edge flaps (ref. 30).

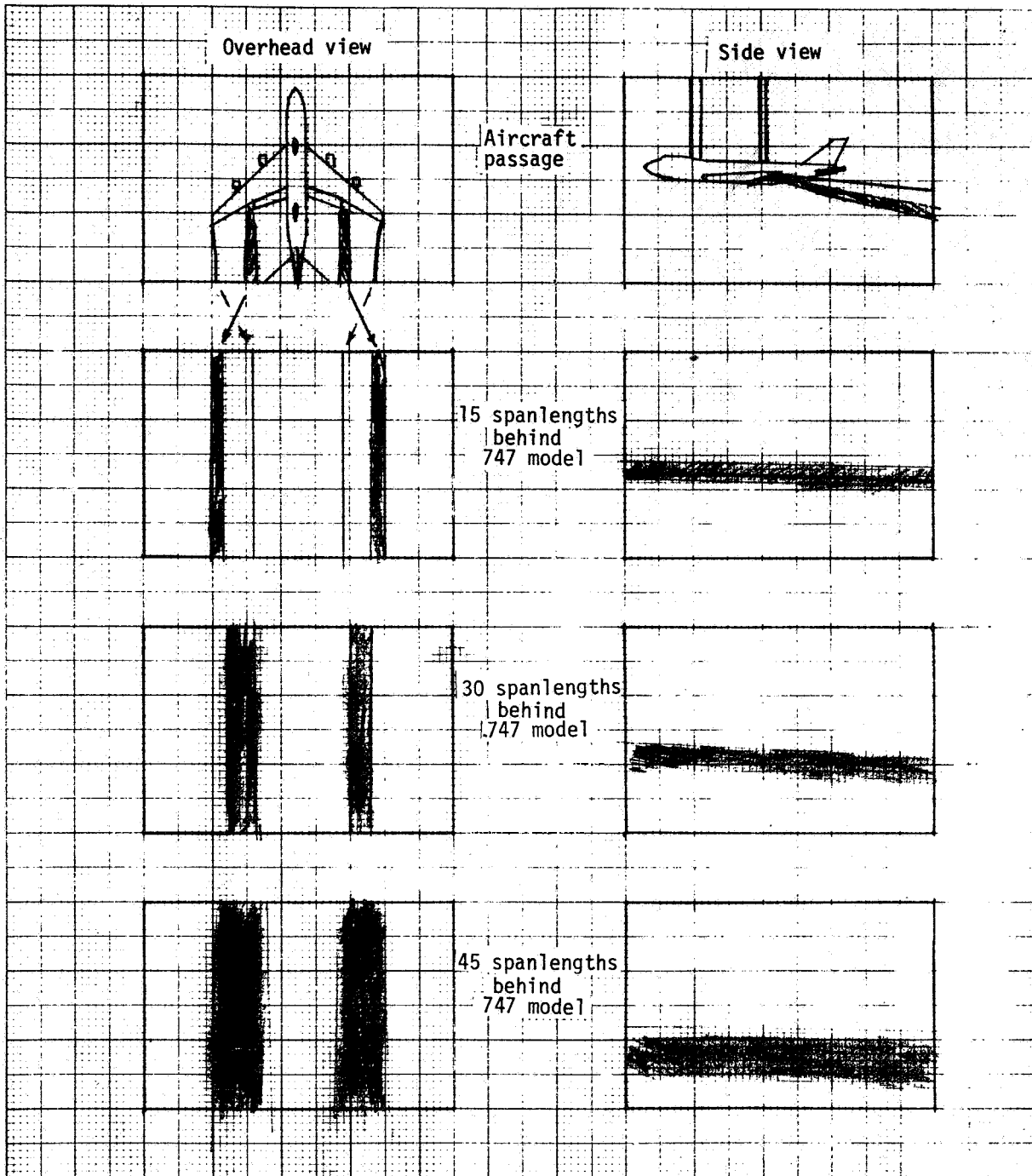
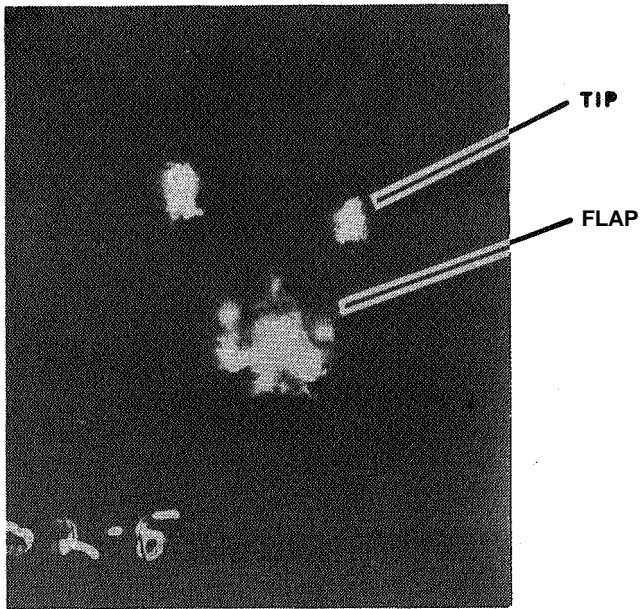
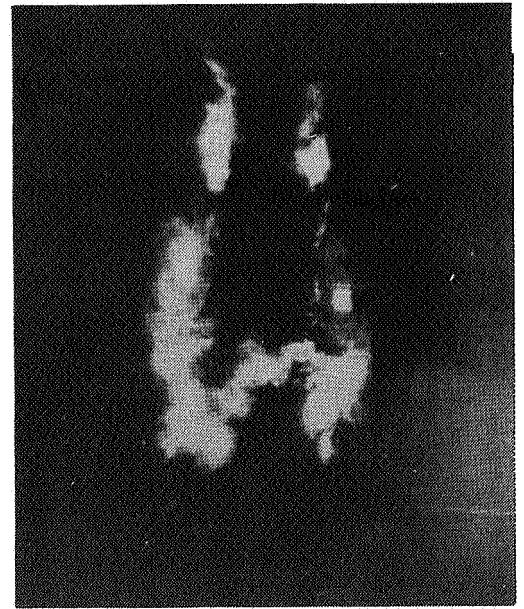


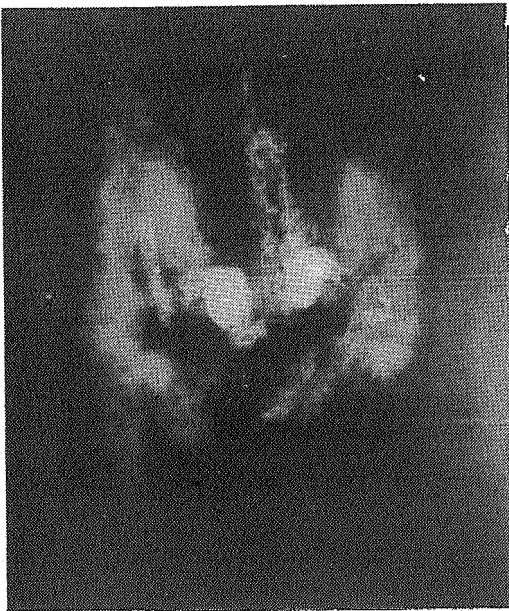
Figure 6.- Illustration of the merger of the wingtip and flap outboard vortices for the 30°/0° flap configuration, as observed in the Hydronautics Inc. water-tow facility (ref. 9).



$x/b_g = 1.5$



$x/b_g = 6$



$x/b_g = 13$



$x/b_g = 32$

Figure 7.--Light slit photographs of dye traces in the water tow facility, generator flaps: $Ldg/0^\circ$, $\alpha = 5.8^\circ$, $U_\infty = 1$ m/sec (3.3 ft/sec).



FLAPS: 30°/30°



FLAPS: 30°/0°

Figure 8.- Photographs of smoke trails from the *B-747* test airplane showing the vortex interactions from reference 31.

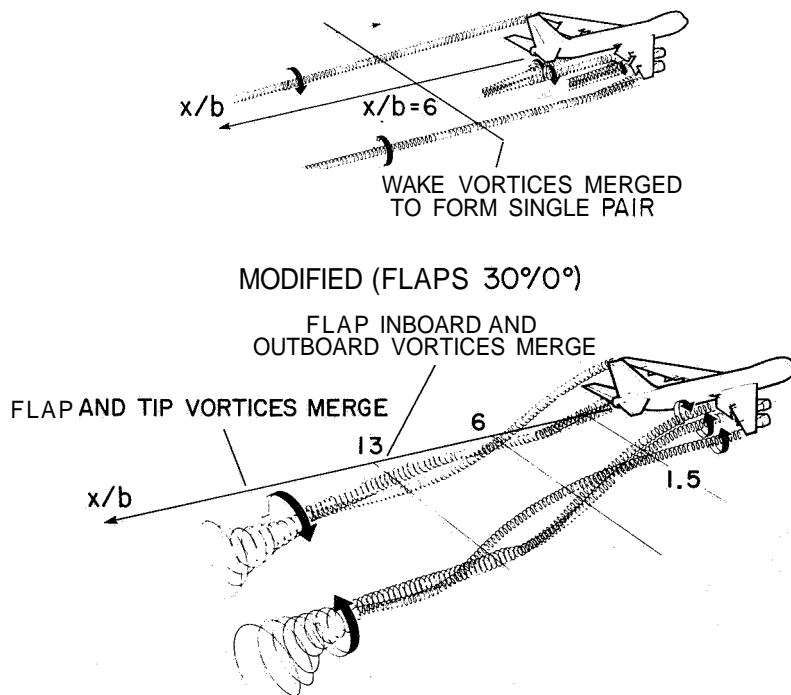


Figure 9.- Sketch of the interaction of the various vortices in the wake of the *B-747* model for the 30°/30° and 30°/0° flap configurations.

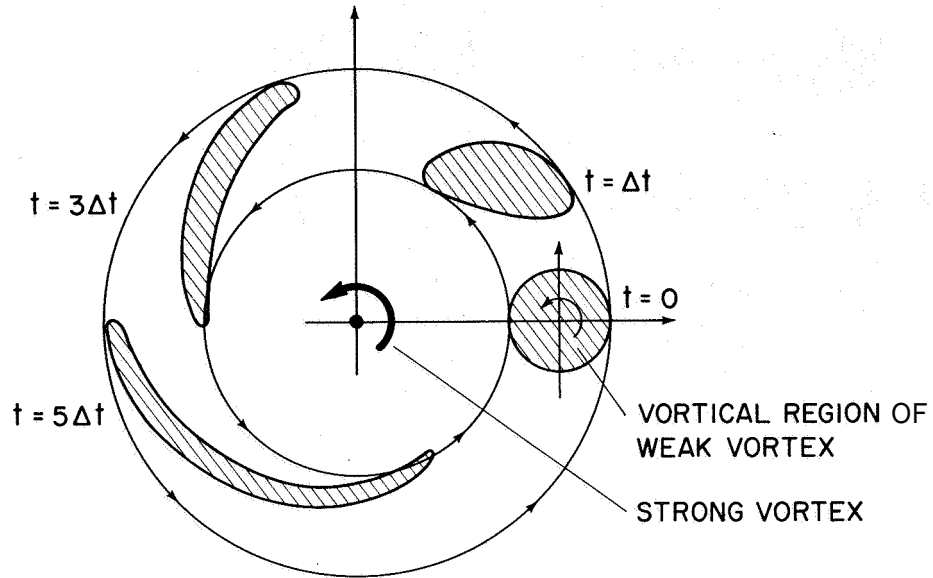


Figure 10.- Sketch of the idealized convective merging of a weak vortex with a strong one.

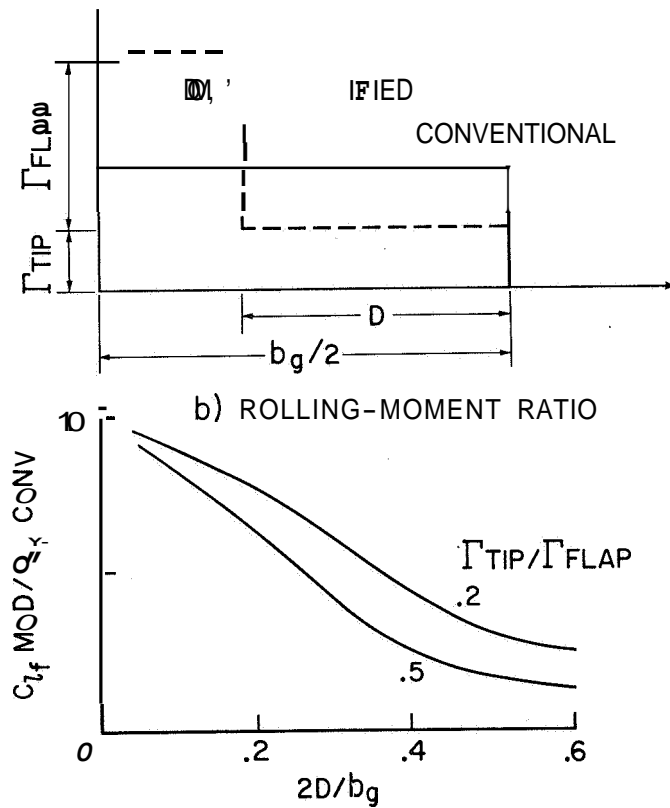


Figure 11.- Idealized example of the effect of merging two vortices into a single Rankine vortex on the rolling-moment coefficient on a follower as compared to a single vortex wake at the same lift and span; $b_f/b_g = 0.2$.

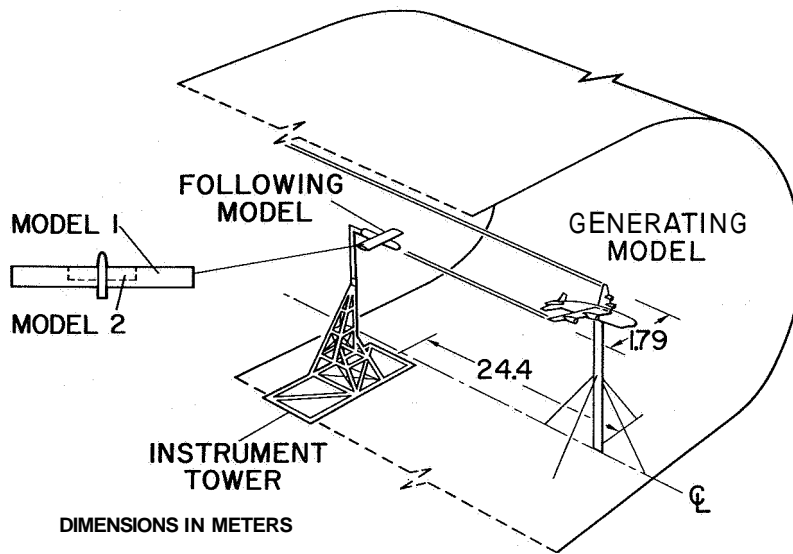


Figure 12.- Experimental setup in the Ames 40- by 80-Foot Wind Tunnel.

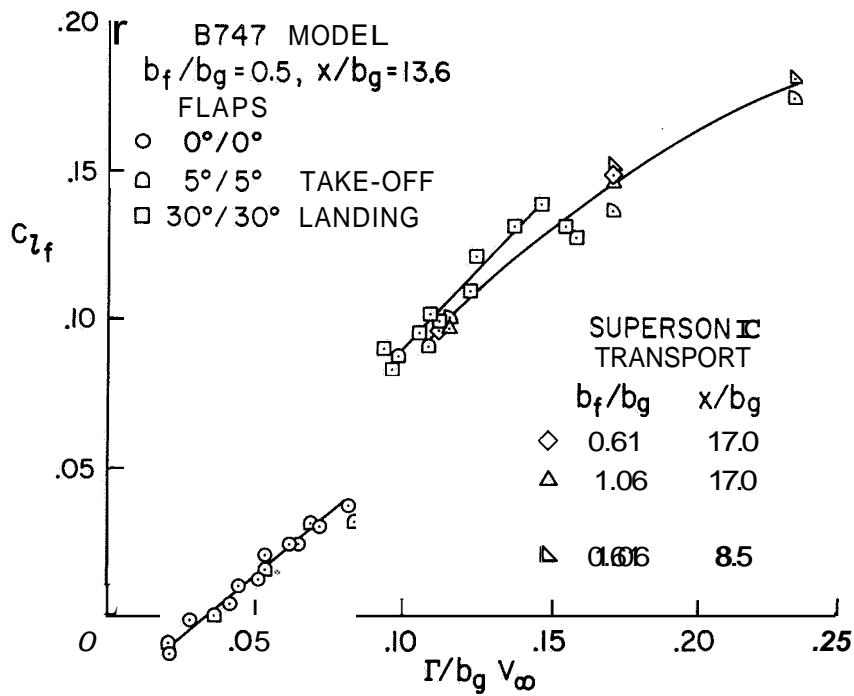
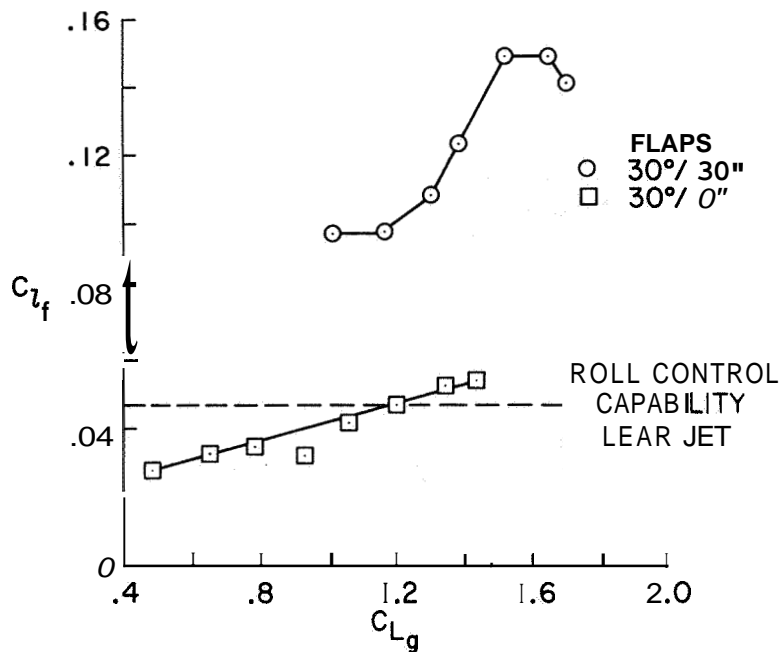
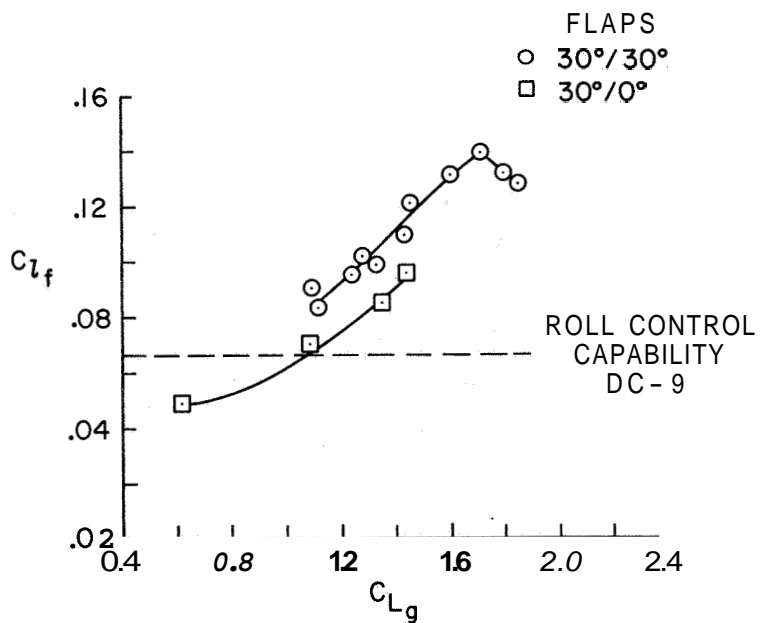


Figure 13.- Variation of the peak rolling-moment coefficient on the following models for the B-747 model with conventional flap settings (ref. 30) and for a supersonic transport model with flaps undeflected (ref. 34), as measured in the Ames 40- by 80-Foot Wind Tunnel.

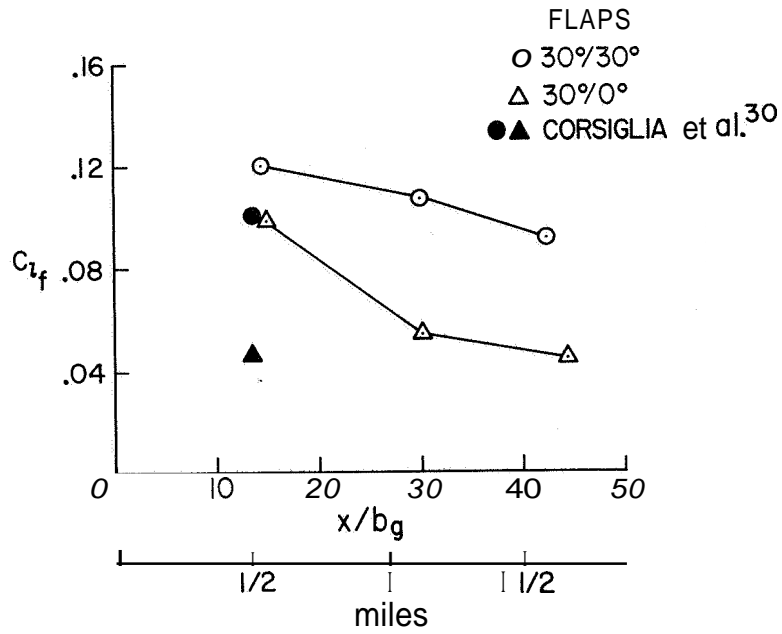


(a) $x/b_g = 13$, $b_f/b_g = 0.2$, Learjet size follower, Ames 40- by 80-Foot Wind Tunnel (ref. 30).

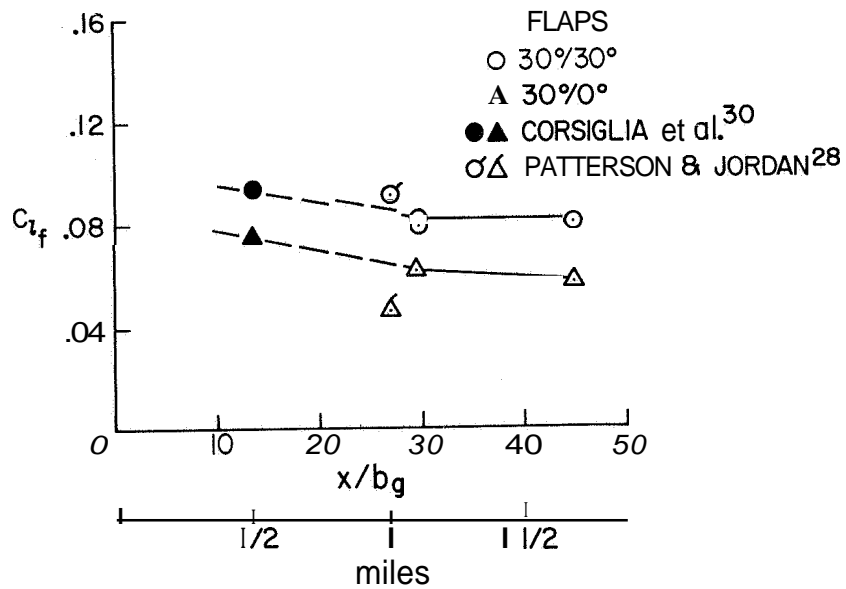


(b) $x/b_g = 13$, $b_f/b_g = 0.5$, DC-9 size follower, Ames 40- by 80-Foot Wind Tunnel (ref. 30).

Figure 14.- The effect of retracting the outboard flap of the B-747 model on the rolling moment imposed on the following model, landing gear up.

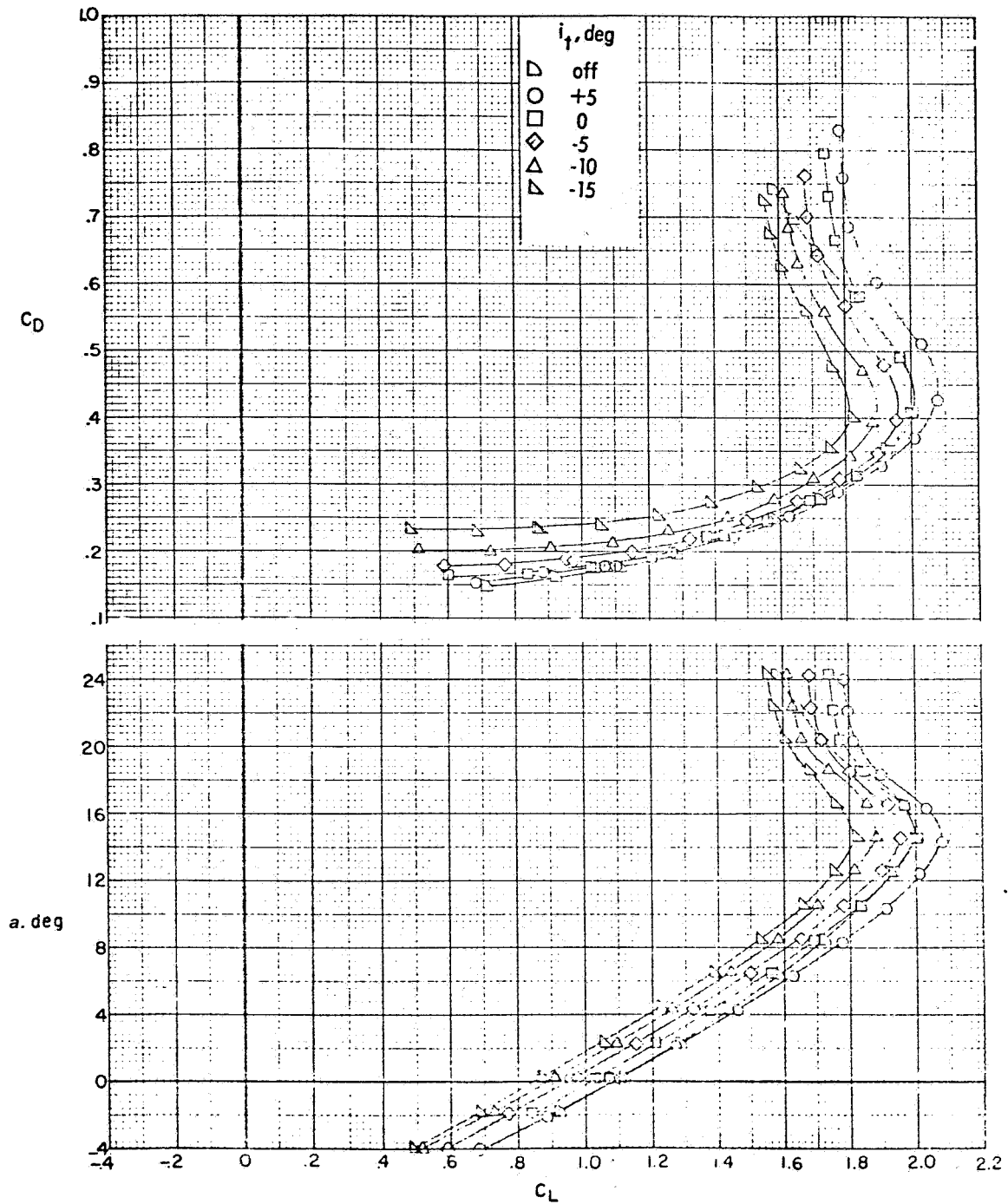


(c) $C_{L_g} = 1.2$, $b_f/b_g = 0.2$, Learjet size follower, Hydronautics Inc. water-tow facility.



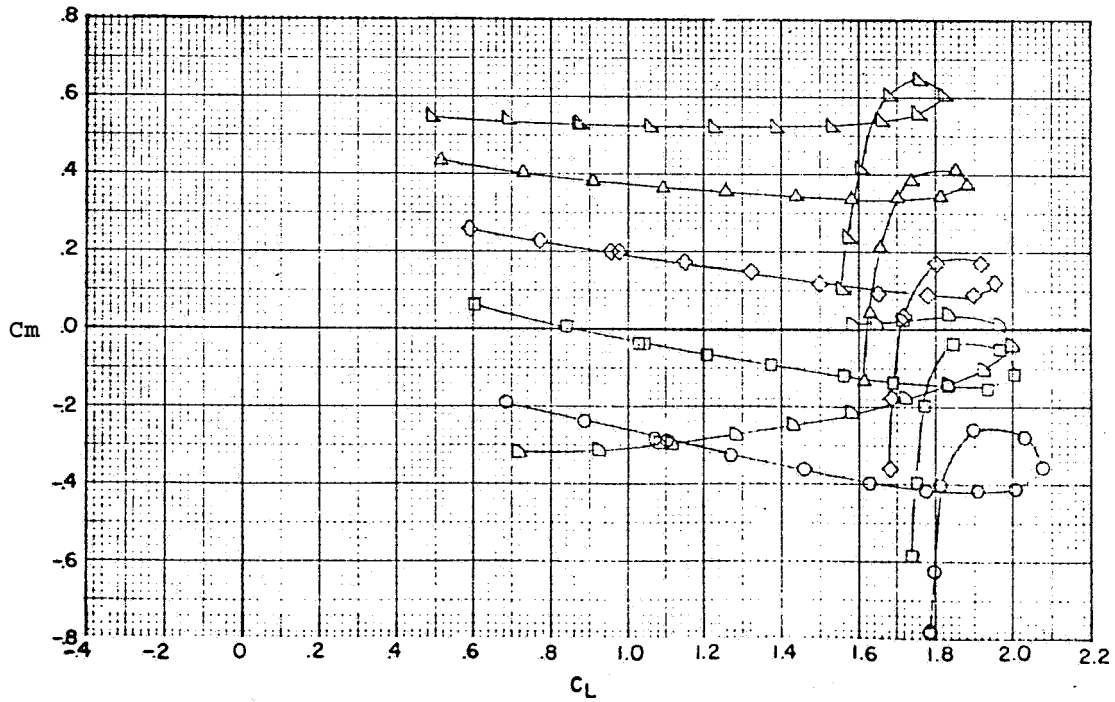
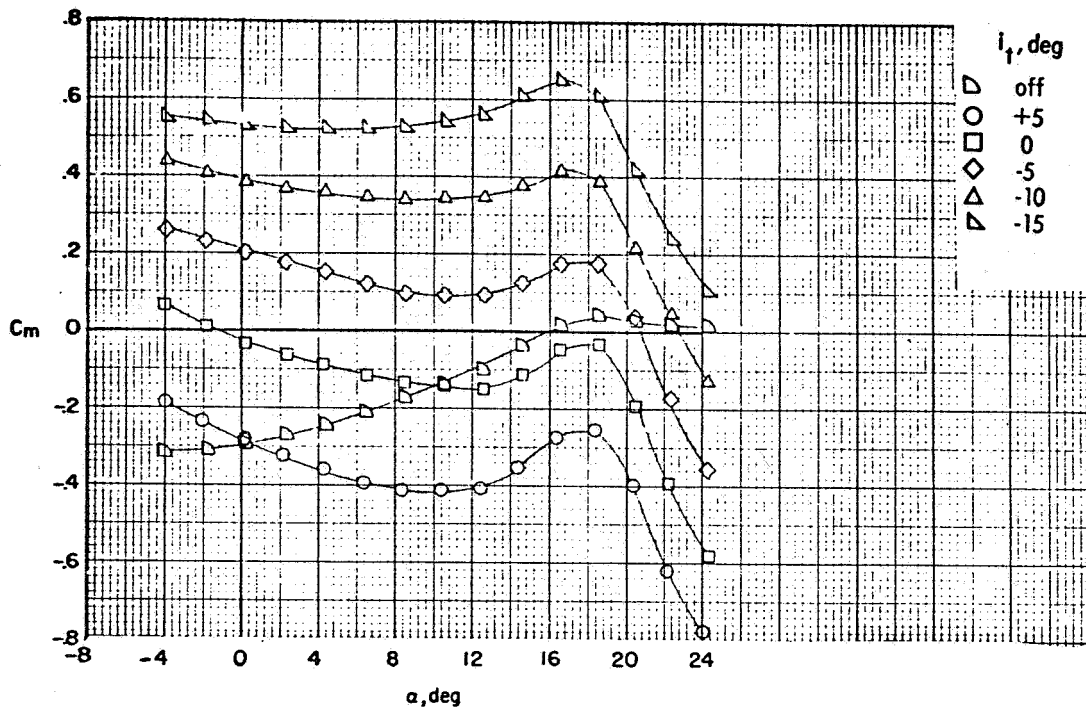
(d) $C_{L_g} = 1.2$, $b_f/b_g = 0.5$, DC-9 size follower, Hydronautics Inc. water-tow facility.

Figure 14.- Concluded.



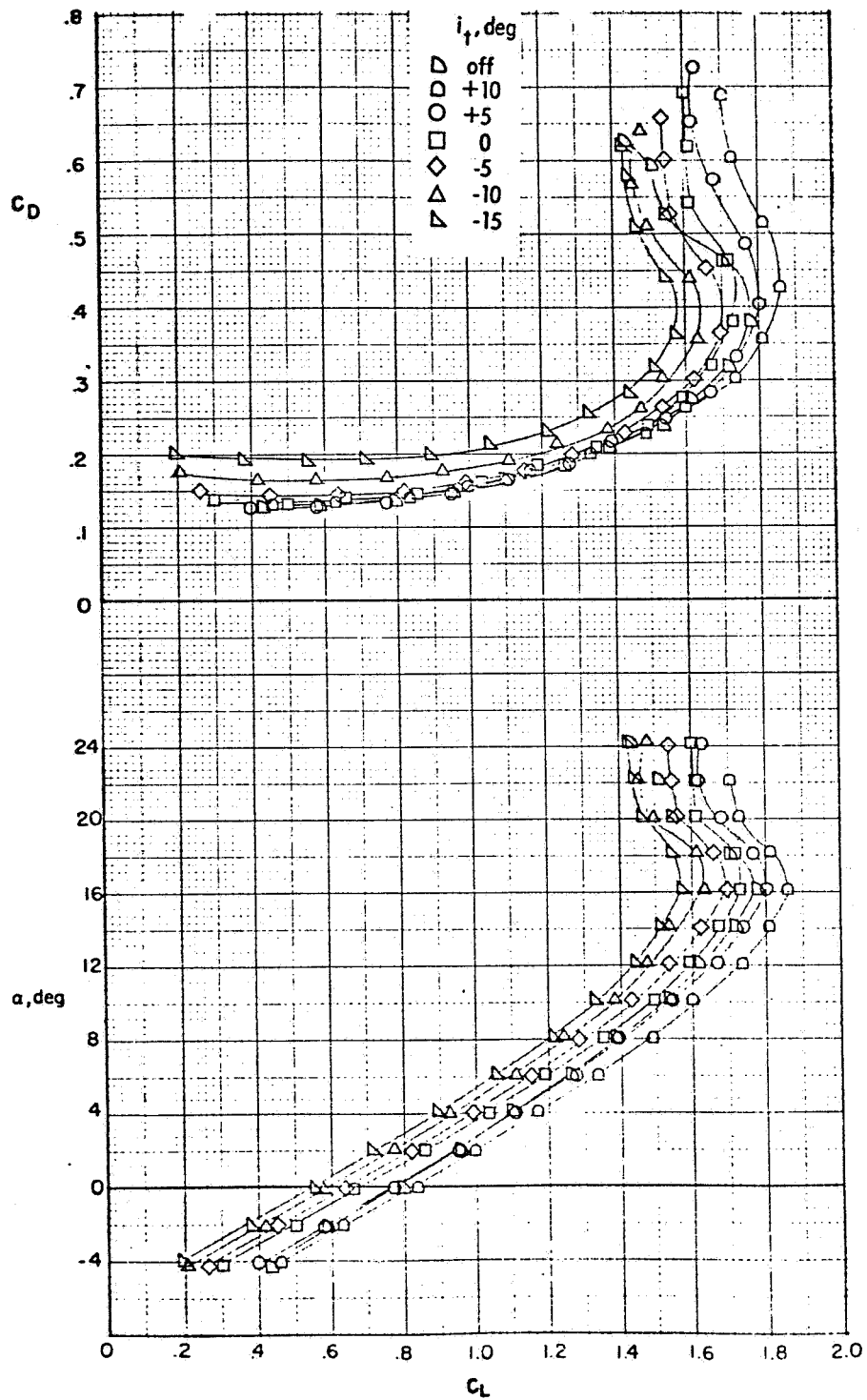
(a) Drag coefficient and angle of attack, flaps 30°/30°, conventional landing configuration.

Figure 15.— Effect of the horizontal-tail incidence on the longitudinal aerodynamic characteristics of the B-747 model, as measured in the Langley V/STOL Wind Tunnel; landing gear up (ref. 14). Moment center at 25 percent mean aerodynamic chord.



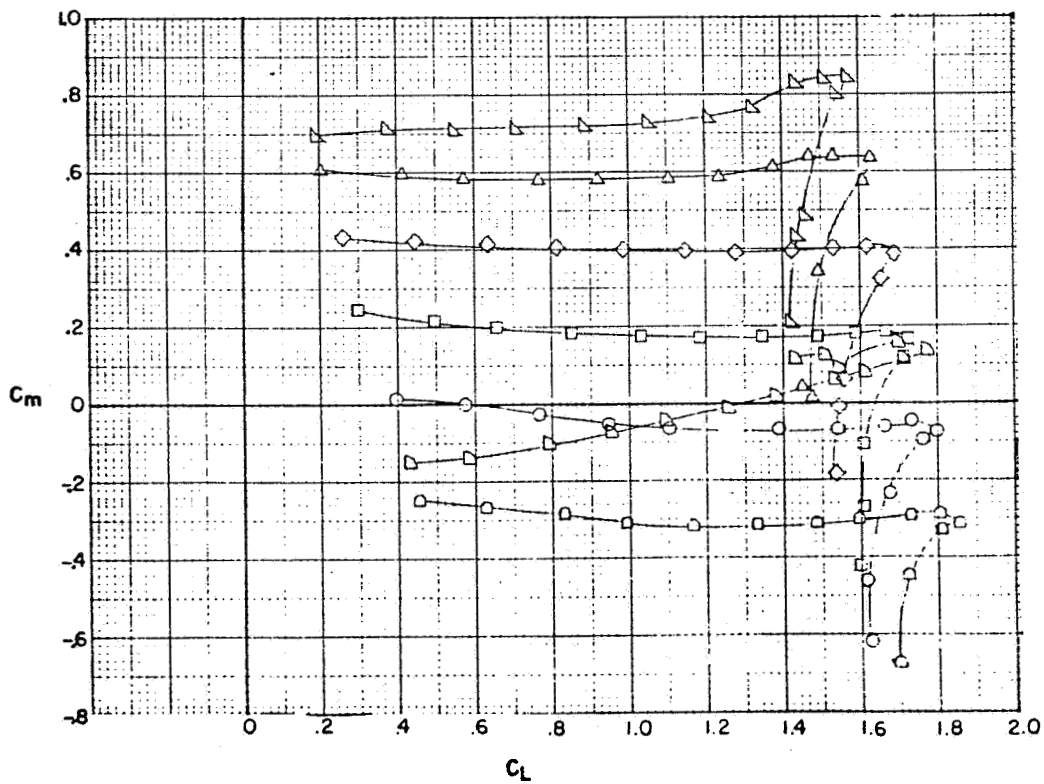
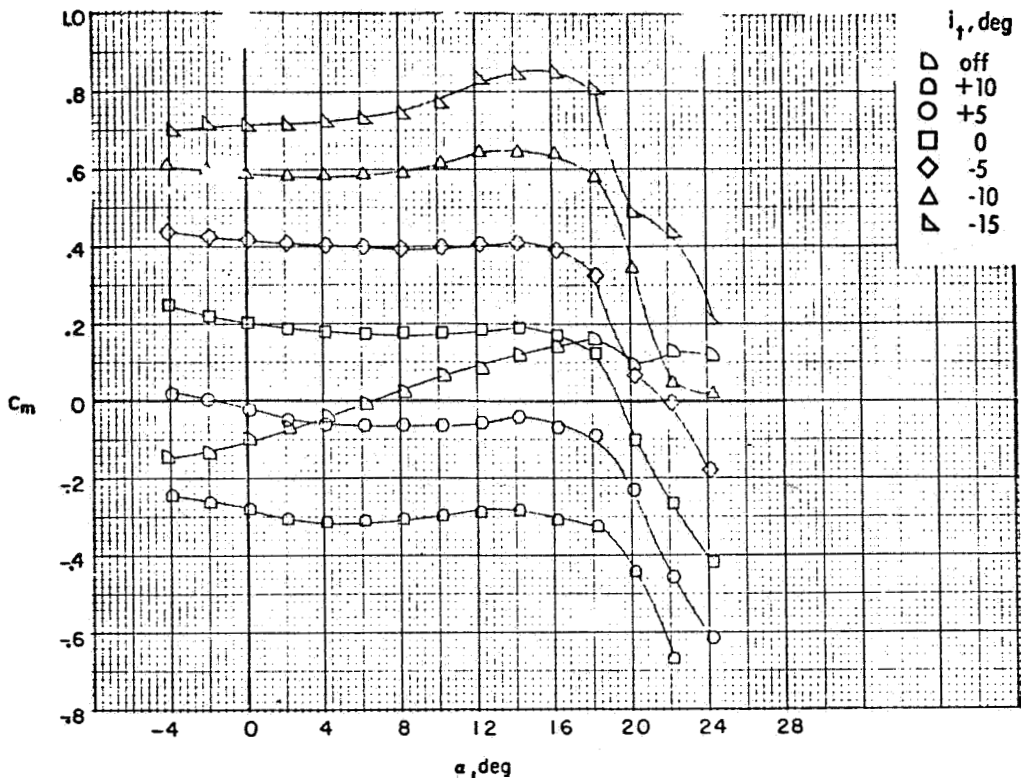
(b) Pitching-moment coefficient, flaps 30°/30°, conventional landing configuration.

Figure 15.- Continued.



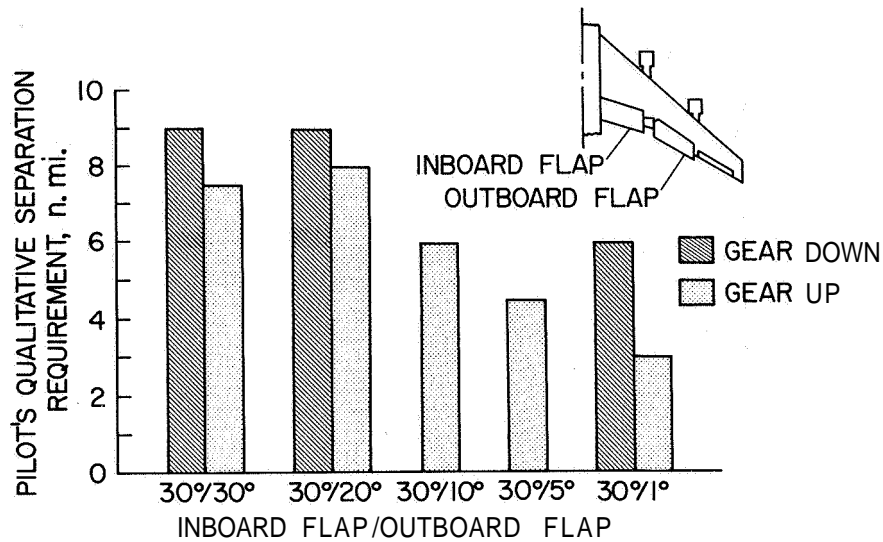
(c) Drag coefficient and angle of attack, flaps $30^\circ/0^\circ$,
outboard flap retracted.

Figure 15.- Continued.

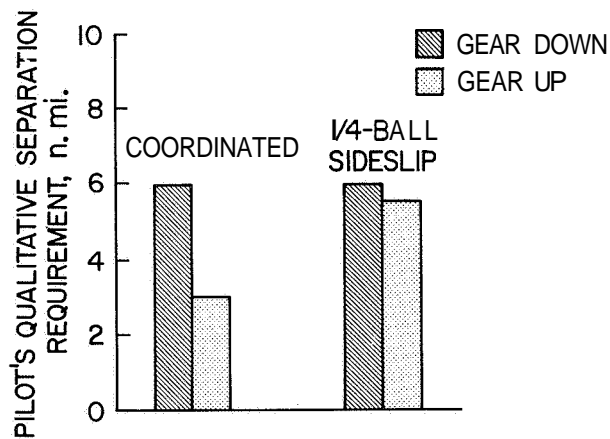


(d) Pitching-moment coefficient, flaps 30°/0°, outboard flap retracted.

Figure 15.- Concluded.

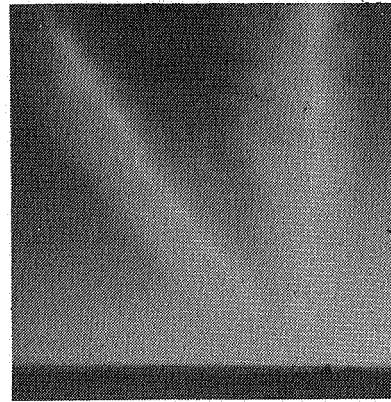
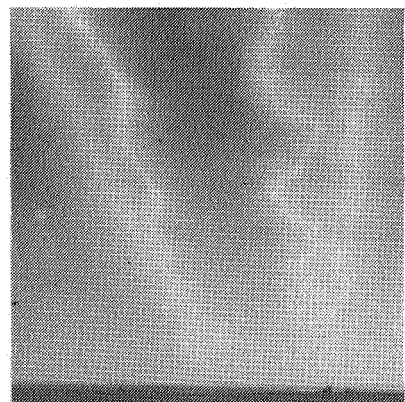
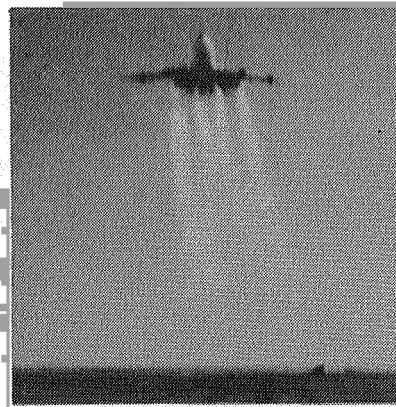


(a) Variation with outboard flap deflection, no yaw.



(b) Variation with yaw on the generator airplane, flaps 30°/1°.

Figure 16.- Pilot qualitative separation requirement for a Learjet or T-37B airplane following a B-747 airplane; level flight (ref. 35).



↑ \approx 15 sec

LANDING GEAR UP

LANDING GEAR DOWN

Figure 17.- Flow visualization photographs from flight tests of the *B-747* airplane in the $30^\circ/1^\circ$ configuration showing the effect of the landing gear on the flap inboard vortices (ref. 31).

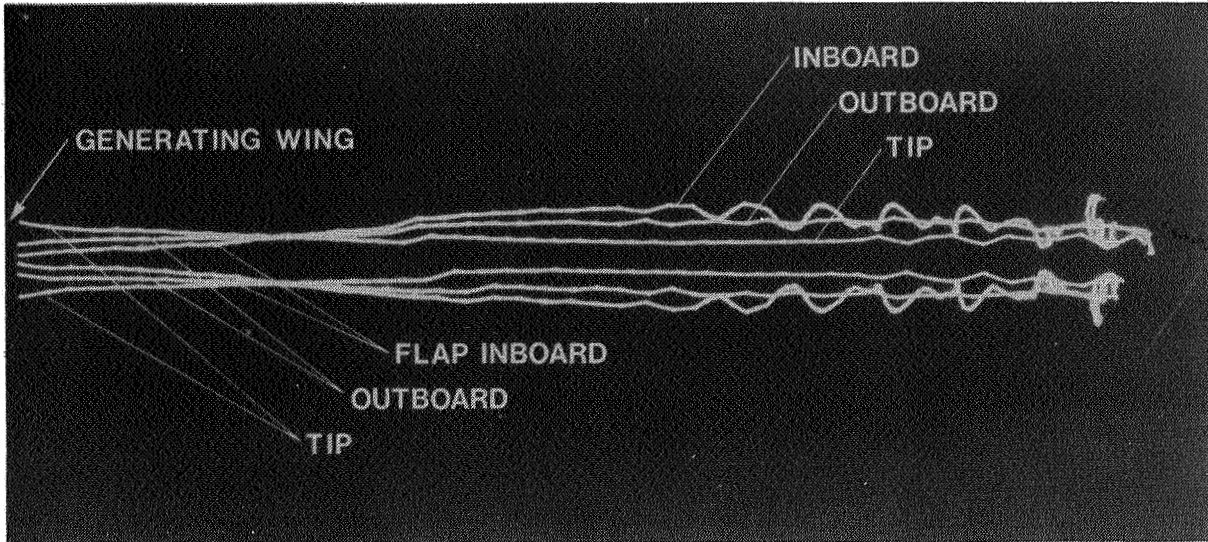


Figure 18.- Computer graphics display of the results of a three-dimensional time-dependent inviscid calculation of the wake vortex interaction behind a configuration with a three vortex pair wake with landing gear up (ref. 36).

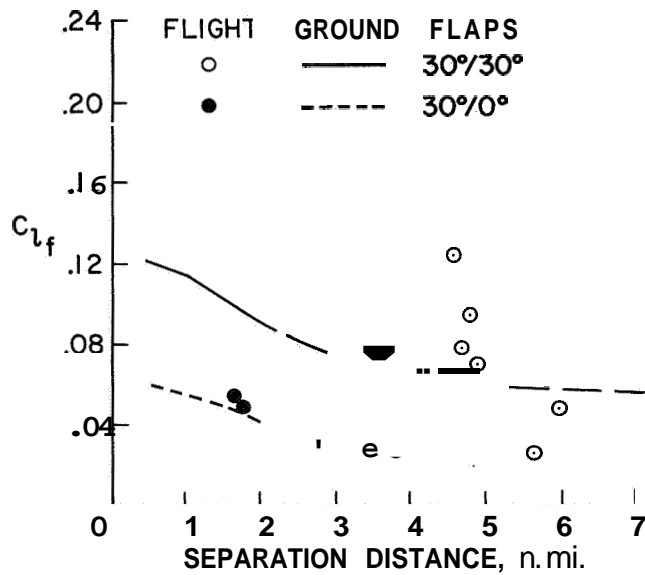


Figure 19.- Comparison of the flight-measured rolling-moment coefficient imposed on the T-37B airplane with the ground-based measured values from reference 32.

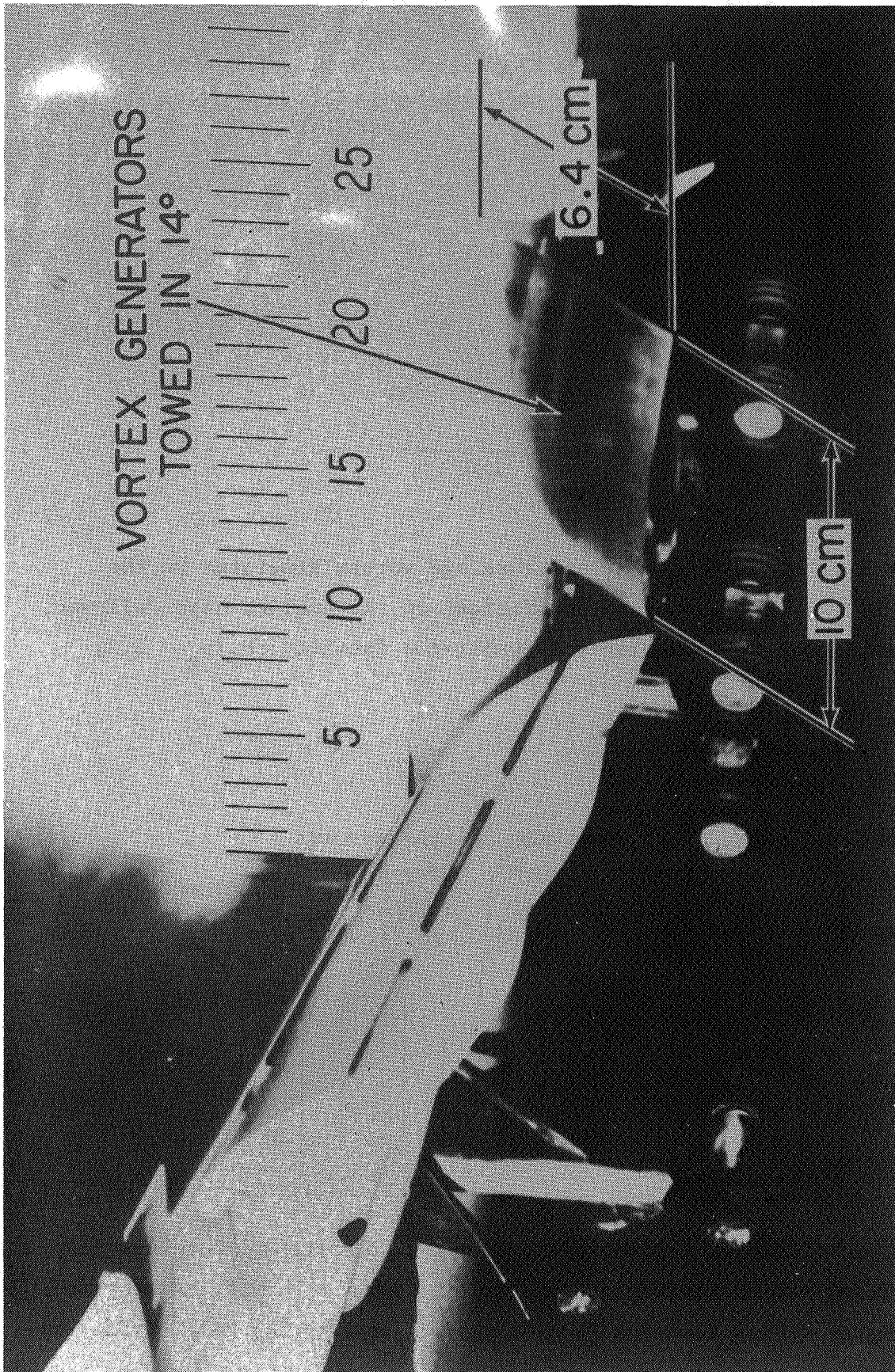


Figure 20 - Photograph of the B-747 model used in the Hydroaerodynamics Inc. water-tow facility tests the fuselage vortex generator (dimensions in cm).

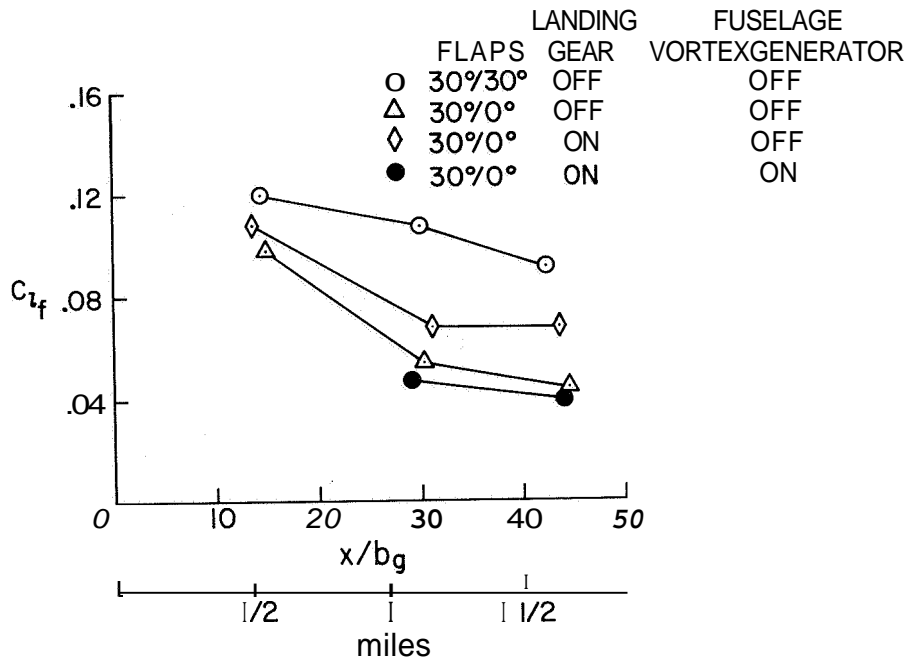


Figure 21.- Effect of landing gear and fuselage vortex generator on the variation of the rolling-moment coefficient on the Learjet size follower, as measured in the Hydronautics Inc. water-tow facility; $b_f/b_g = 0.2$, $C_{L_g} = 1.2$.

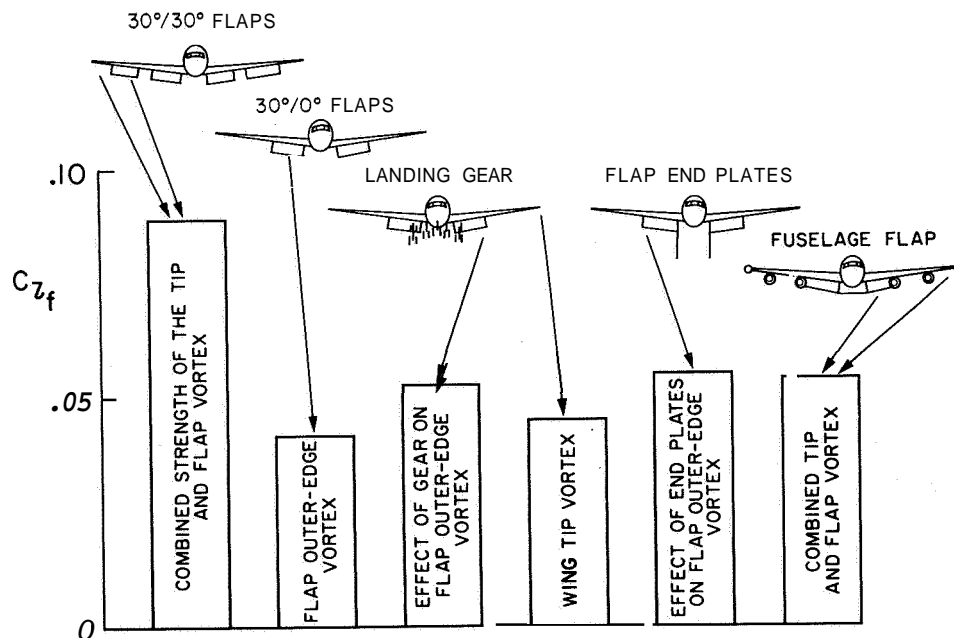


Figure 22.- The effects of landing gear, flap end plates, and fuselage flap on the rolling-moment coefficient on the DC-9 size follower, as measured in the Langley Vortex Research Facility; $b_f/b_g = 0.5$, $C_{L_g} = 1.2$ (ref. 28).